Single-cell detection using a thin film transistor photosensor with micro-partitions

Tsuyoshi Tanaka, Yoshihiko Sunaga, Keiichi Hatakeyama and Tadashi Matsunaga*

Received 20th May 2010, Accepted 24th June 2010
DOI: 10.1039/c0lc00039f

A thin film transistor (TFT) photosensor was applied to single-cell detection by identifying cell surface molecules based on chemiluminescence. Micro-partitions were directly fabricated on the TFT photosensor surface by photolithography. The surface of each pixel was surrounded by 25 μm-height partitions, forming areas of approximately 30 μm × 30 μm for cell entrapment and photosensing. Visualization of individual JM cells, stained with mouse anti-human CD8 IgG1 primary antibody and Horseradish peroxidase (HRP)-labeled anti-mouse IgG1 secondary antibody, as bright-pixels was successfully achieved using the micro-partitioned TFT photosensor integrated into a microfluidic chamber. Furthermore, real-time monitoring of HRP-labeled JM cells was also accomplished. The fabrication of micro-partitions on the surface of the TFT photosensor allows highly efficient single-cell entrapment and chemiluminescence-based detection of JM cells. This is the first report of single-cell entrapment and subsequent signal detection on the photosensing area of individual pixels of TFT photosensor. This system will allow high-throughput and real-time analysis of more than 10^4 cells with minimum optical system requirements.

Introduction

Flow cytometry is a powerful tool that has been widely used for high-throughput analysis of cells based on morphology and surface markers.[1–8] In particular, the surface molecules of blood cells have been classified into over 300 types of clusters of differentiation (CDs). Consequently, flow-cytometric identification of blood cells based on CDs has been commonly employed not only in basic research but also for clinical diagnostic applications such as lymphocyte subset analysis,[9] leukemia typing,[10] and $CD34^+$ cell counting.[11]

Recently, miniaturized cytometers (on-chip cytometers) have been proposed for portable applications. Two types of detection formats are used in on-chip cytometers; flow-based analysis, which is recognized as a miniaturized flow cytometer, and non-flow-based analysis, which employs two-dimensional image analysis. Flow-based analysis allows the reduction of sample volume and the downsizing of fluidic and optical systems. Target cells are guided to a detection point in the microchannel by microfluidic flow, as in a conventional flow cytometer, and light signals derived from the cells are detected by the optical components, *i.e.*, photomultiplier tubes (PMTs) and charge coupled device (CCD) camera.[12–14] In contrast, in non-flow-based analysis target cells are pre-entrapped and pre-assembled at a single-cell level on a microwell array,[15] a microcavity array,[16,17] or an array of micromechanical traps[18] and subsequently analyzed by fluorescent microscopy. Non-flow-based approaches enable the monitoring of time-dependent changes in groups of cells and the collection of specific cells. In both analytical systems, flow channels and array devices for cell analysis are integrated into miniaturized chips. However, further downsizing and reduction in price of these systems is limited because the devices still require external optical detection systems including PMTs or fluorescent microscope.

For the last few years, a lens-free photodetection system that enables cell analysis with a wide range of observation areas and minimum optical system requirements has attracted much attention. In this assay format, target cells are placed directly on the surface of miniaturized and portable photosensor *e.g.* a CCD and complementary metal-oxide semiconductor (CMOS) image sensor. The light signals derived from individual cells are detected by the photosensor without lenses. High-throughput cell analysis using a photosensor has been reported by Ozcan *et al.*[19–22] The different morphologies of red blood cells and yeast cells were successfully distinguished based on comparison of the diffraction patterns of individual cells generated by the irradiation of monochromatic light. This approach has the advantage of being smaller in size, requiring a less expensive optical detection system, and permitting high-throughput cell analysis.

Our group has demonstrated a novel DNA chip device using a thin film transistor (TFT) photosensor based on lens-free photodetection.[23,24] The surface of the TFT photosensor was coated with TiO_2 for the fabrication of an optical filter which cut the wavelength to shorter than approximately 300 nm. Oligonucleotides were directly immobilized on the sensor surface and light signals derived from DNA-DNA hybridization were detected by the sensor as circular spots based on fluorescence under UV irradiation (289 ± 10 nm).[23] Furthermore, chemiluminescent detection had superior signal-to-noise ratio to fluorescent detection.[24] In chemiluminescent detection, an external light source for excitation is unnecessary, resulting in downsizing and reduction in price. In this study, the TFT photosensor was applied to single-cell detection by identifying cell surface

Department of Biotechnology, Tokyo University of Agriculture and Technology, 2-24-16, Naka-cho, Koganei, Tokyo, 184-8588, Japan. E-mail: tmatsuna@cc.tuat.ac.jp; Fax: +81-42-385-7713; Tel: +81-42-388-7020

molecules based on chemiluminescence. Microstructures, named "micro-partitions", were fabricated on the TFT photosensor surface by photolithography to permit entrapment of individual cells on single pixels. Detection of JM cells, human T-cell line, was carried out by identification of the cell surface marker CD8, which has been used as a measure of HIV infection.[9] Furthermore, real-time monitoring of JM cell population based on luminescent intensity measurements was demonstrated.

Experimental

Materials

Biotin-labeled polystyrene particles (15.3 μm in diameter) were purchased from Spherotech, Inc. (Lake Forest, IL, USA). Horseradish peroxidase (HRP)-conjugated streptavidin (HRP-SA) and SuperSignal ELISA Femto Maximum Sensitivity Substrate were obtained from Pierce Biotechnology (Rockford, IL, USA). Polymethylmethacrylate (PMMA) was purchased from Mitsubishi Rayon Co., Ltd. (Tokyo, Japan). Sylpot 184 silicone elastomer and curing agent were obtained from Dow Corning Asia, Ltd. (Tokyo, Japan). Mouse anti-human CD8 IgG1 antibody and HRP-labeled anti-mouse IgG1 antibody were obtained from Santa Cruz Biotechnology, Inc. (Santa Cruz, CA, USA). SYBR Green I was obtained from Molecular Probes (Eugene, OR, USA). Other chemicals and organic solvents were purchased from Wako Pure Chemical Industries (Osaka, Japan).

Fabrication of micro-partitions on the surface of the TFT photosensor

An internal-amplification photosensor using a double-gate structure TFT (TFT photosensor) was used as a photosensor. The TFT photosensor consisted of a 200 × 240 pixel array with a 50-μm pitch (sensor area: 10 mm × 12 mm).[23,24] The top gate acts as a photosensing gate, while the bottom gate acts as a pixel selection gate. The photosensing mechanism is the photo-induced gate modulation. Noise cancelling in a-Si was carried out before each sensing process. The TFT photosensor detects light over a broad range of wavelengths, with peak sensitivity at 450 nm.

In order to entrap a single cell on each pixel of the TFT photosensor, micro-partitions were fabricated using photolithography based on two-step UV irradiation. The first irradiation resulted in the formation of the outer frame and the second irradiation formed the micro-partitions (Fig. 1). First, the TFT photosensor was baked at 150 °C for 20 min to dehydrate the sensor surface. Then, an SU-8 sheet (thickness: 25 μm; Micro-Chem Corp., Newton, MA, USA) was adhered to the surface of the photosensor by baking at 95 °C for 5 min. After removal of the SU-8 protective film, the photosensor was baked at 95 °C for 10 min again to enhance adhesion. Subsequently, UV light was irradiated (first irradiation) from the top side of the photosensor using a mask aligner (MA-10; MIKASA Co. Ltd., Tokyo, Japan) for 25 s to form an outer frame, using a black PMMA substrate as a photomask. UV light was then irradiated (second irradiation) from the bottom side of the photosensor for 100 s to generate a unique photoresist pattern. The UV light passed only through the gaps between the photosensor pixels. After UV irradiation, the photosensor was baked at 65 °C for 5 min and then at 95 °C for 15 min to promote a polymerization reaction.

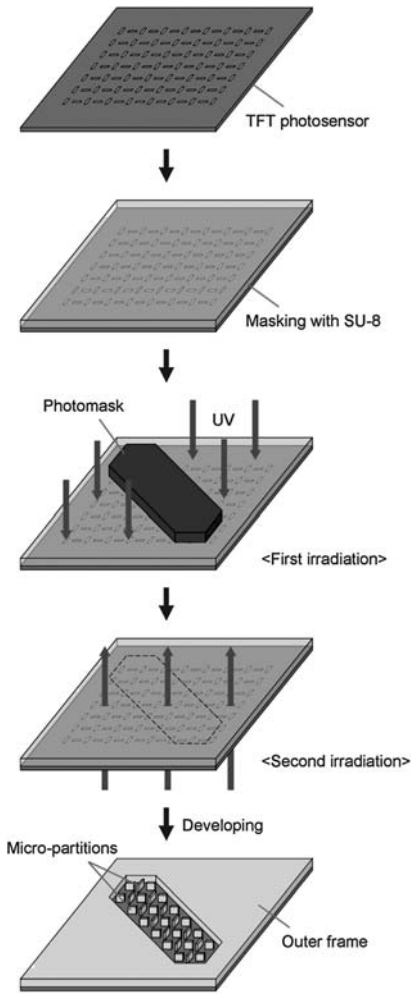

Fig. 1 Fabrication procedure for micro-partitions on the TFT photosensor surface by photolithography.

Subsequently, the photosensor was immersed in SU-8 developer (MicroChem Corp.) for 200 s and rinsed with distilled water to remove the non-irradiated area of SU-8. After development, the photosensor was baked at 150 °C for 20 min. The cured SU-8 microstructures on the TFT photosensor were observed by scanning electron microscopy (SEM; VE-9800; KEYENCE, Osaka, Japan).

Visualization of HRP-labeled polystyrene particles using the TFT photosensor

HRP-labeled polystyrene particles (HRP-particles) were prepared by mixing biotin-labeled polystyrene particles and HRP-SA as follows; a 100 μl-suspension of biotin-labeled polystyrene particles was added to 500 μl of 5 μg ml^{-1} HRP-SA and incubated with continuous shaking for 30 min at room temperature. To remove excess HRP-SA, the HRP-SA and biotin-labeled polystyrene particle complexes were washed three times with phosphate-buffered saline (PBS; 11.8 mM phosphate buffer, 137 mM NaCl, pH 7.4) by centrifugation (10,000*g*, 4 °C, 5 min) and resuspended in 100 μl of PBS. A sealed chamber (Frame-Seal Incubation Chambers for In Situ PCR and Hybridization;

9 mm × 9 mm; Bio-Rad, Hercules, CA, USA) was adhered to the surface of the TFT photosensor. Subsequently, 10% Blockmaster CE510 (JSR Corporation, Tokyo, Japan) solution was applied to the chamber and incubated for 1 h at room temperature. The chamber was rinsed with PBS using a micropipette and 5 μl of HRP-particle suspension were added to 100 μl of substrate solution (SuperSignal ELISA Femto Maximum Sensitivity Substrate). Subsequently, 25 μl of the suspension was applied to the detection chamber and a coverslip was introduced. After 5-min incubation, the chemiluminescent signals of HRP-particles were detected using the TFT photosensor. In parallel, microscopic observation of the particles on the photosensor was performed using a digital microscope (VHX-100, KEYENCE) to confirm the particles' position.

Fabrication of a microfluidic chamber on the TFT photosensor

A microfluidic chamber of polydimethylsiloxane (PDMS) and a PMMA clamp were fabricated (Fig. 2). PMMA was also used as a mold for the production of the PDMS chamber. The PMMA master mold was produced using the CAD/CAM system (Roland DG, Shizuoka, Japan). The PDMS chamber was fabricated by pouring a mixture of Sylpot 184 silicone elastomer and curing agent (10 : 1) onto the master mold, followed by degassing with a vacuum pump and curing for at least 2 h at 75 °C. The cured PDMS chamber, including a microfluidic channel (width: 3 mm, height: 100 μm), was carefully peeled off the mold. Subsequently, the PDMS chamber and the TFT photosensor with micro-partitions were exposed to oxygen plasma at an air flow rate of 40 ml min^{-1} for 40 s and put in contact with each other (Fig. 2A and B). The PDMS chamber was then clamped with the PMMA clamp and connected to a syringe pump (KD Scientific, Holliston, MA, USA) with PEEK tubes and silicon tubes (Fig. 2C and D). The microfluidic chamber on the TFT photosensor was pretreated with 20% Blockmaster CE510 solution by incubation for 60 min.

Chemiluminescent detection of JM cells using the TFT photosensor

JM cells, human T-cell line, were cultured in RPMI 1640 medium (Sigma-Aldrich, Irvine, UK) containing 10% (v/v) fetal bovine serum (FBS; Invitrogen Corp., Carlsbad, CA, USA) and 1% (v/v) penicillin/streptomycin (Invitrogen Corp.) at 37 °C with 5% CO_2 supplementation for 3 to 4 days. Cells were then stained with primary antibody and HRP-labeled secondary antibody for chemiluminescent detection. Suspensions of cultured cells were centrifuged at 300*g* for 5 min at 4 °C and resuspended in PBS at a concentration of 1 × 10^6 cells ml^{-1}. Mouse anti-human CD8 IgG1 antibody (2 μg ml^{-1}) was added to the cell suspension and incubated at 4 °C for 30 min. After removal of excess primary antibody by centrifugation, HRP-labeled anti-mouse IgG1 secondary antibody (0.4 μg ml^{-1}) was added and incubated at 4 °C for 30 min. After removal of excess secondary antibody, the stained JM cells were introduced into the TFT photosensor integrated into the microfluidic chamber (microfluidic TFT photosensor). The flow rate was set at 1.8 μl min^{-1} using a syringe pump. After washing with PBS at a rate of 1.8 μl min^{-1} to flush out untrapped cells, chemiluminescent substrate solution was introduced into the microfluidic chamber at a rate of 1.8 μl min^{-1}.

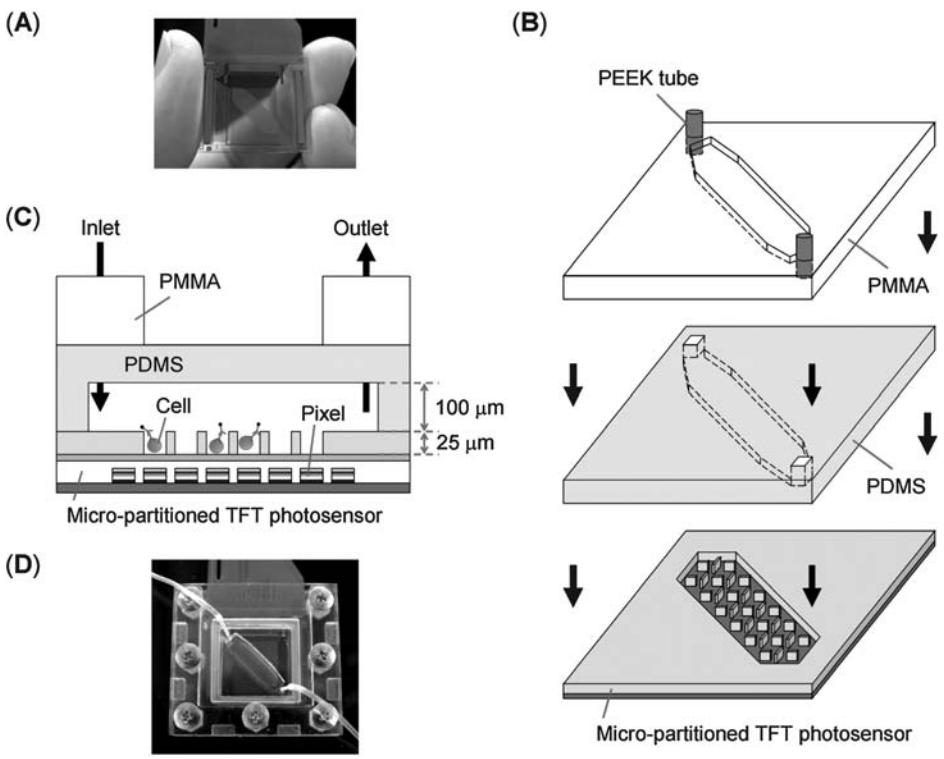

Fig. 2 (A) Photograph of micro-partitioned TFT photosensor. (B) Fabrication of microfluidic chamber on the TFT photosensor. (C) Side sectional view of microfluidic chamber. (D) Photograph of microfluidic chamber on the TFT photosensor.

The chemiluminescent signals from the JM cells were detected every 30 s using the TFT photosensor with constant introduction of the substrate solution. To confirm the positions of JM cells on the photosensor, fluorescent microscopic observation was performed (BX61; Olympus Corp., Tokyo, Japan). For microscopic observation, JM cells were stained with 5× SYBR Green I solution at 4 °C for 15 min before the antibody staining process.

Signal processing

The luminescent signal was digitized and visualized for two-dimensional imaging (8 bit, BMP format).[23,24] Images were captured at an exposure time of 4.8 or 21.0 s. Background images were also measured just before the introduction of the luminescent sources onto the TFT photosensor. Background images were subtracted from raw images to remove background signals at each pixel.

Results and discussion

SEM of TFT photosensor before and after fabrication of micro-partitions

To achieve efficient signal detection from the cell surface, individual cells should be correctly positioned on each pixel of the TFT photosensor. Therefore, microfabrication of the surface of the TFT photosensor was performed. Fig. 3 shows the SEM images of the TFT photosensor surface before and after microfabrication. The untreated surface of the TFT photosensor was nearly flat, although a regular wiring pattern was observed (Fig. 3A). The area surrounded by the dotted line in Fig. 3A is the photosensing area of a single pixel. Fabrication of micro-partitions was successfully achieved after the photolithography procedure (Fig. 3B). The surface of each pixel was surrounded by 25 μm-height partitions, forming areas of approximately 30 μm × 30 μm for cell entrapment and photosensing.

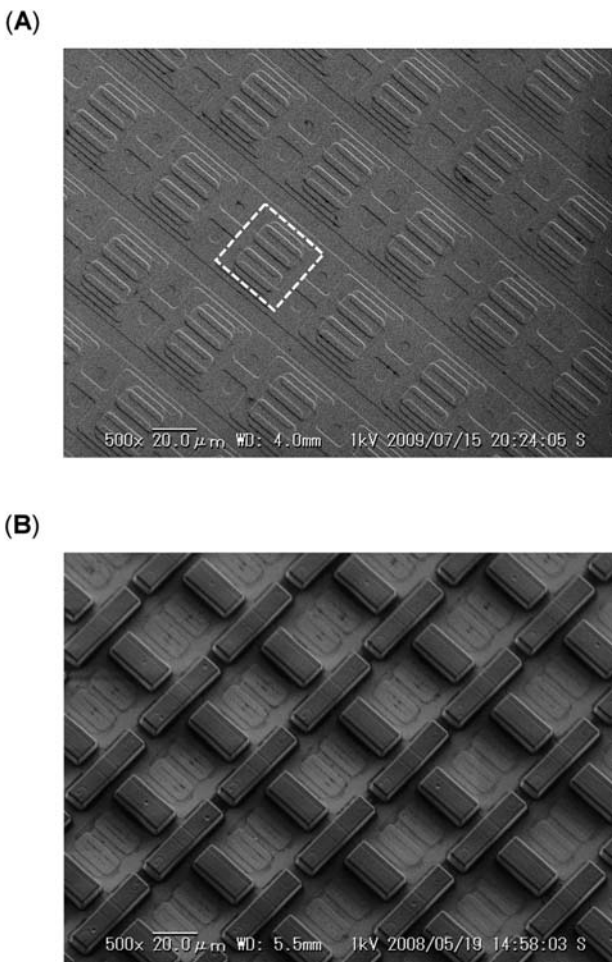

Fig. 3 SEM images of TFT photosensor surfaces in the absence (A) or presence (B) of micro-partitions.

Entrapment and counting of HRP-labeled particles on the surface of the TFT photosensor with and without micro-partitions

To confirm the effect of micro-partitions on cell entrapment, HRP-labeled polystyrene particles (HRP-particles) were chosen to serve as a model for leukocytes and were introduced onto the TFT photosensor surface with and without micro-partitions. The number of particles on the photosensing areas of single pixels was determined by direct particle counting using microscopy. On the micro-partitioned TFT photosensor, 99.9% of the particles were successfully localized on the photosensing areas (Fig. 4A). In contrast, on the untreated TFT photosensor, 48.8% of the particles were not positioned on the photosensing areas (Fig. 4B, white triangles). These results indicate that micro-partitions allow highly efficient entrapment of particles on the TFT photosensor.

The effect of micro-partitions on detection of signals from the HRP-particles was investigated. In our previous work, the detection limit of the TFT photosensor for HRP was 2.5 molecules μm^{-2}, *i.e.*, 2.3×10^3 molecules/photosensing area of a single pixel.[24] Because approximately 2.8×10^6 molecules of HRP can be bound to a single polystyrene particle according to the manufacturer's literature, the photosensor used in this study is sufficiently sensitive to detect each HRP-particle. After deposition of the HRP-particles and substrates on the TFT photosensor, bright- and dark-pixel patterns were visualized in both micro-partitioned and untreated TFT photosensors (Fig. 4C and D). The bright pixels indicate that photoinduced signal transduction has occurred. To examine whether bright signals were derived from HRP-particles, the particle positions were confirmed by microscopic observation (Fig. 4A and C). The positions of bright pixels corresponded precisely to the particle positions when the micro-partitioned TFT photosensor was used; this correlation did not exist when the untreated TFT photosensor was used (Fig. 4B and D). When HRP-particles were positioned on gap spaces, they were recognized by several nearby pixels (Fig. 4B, white triangles).

Fig. 5 shows the histograms of luminescent intensities detected by each pixel on the TFT photosensor. The data include all the signals detected by pixels, whether associated with HRP-particles or not. The luminescent intensities of the HRP-particles are indicated in gray and background signals are indicated in white. The luminescent intensities of the HRP-particles showed a normal distribution and were distinguishable from background signals on the micro-partitioned TFT photosensor (Fig. 5A). In contrast, a broad distribution was observed after plotting the

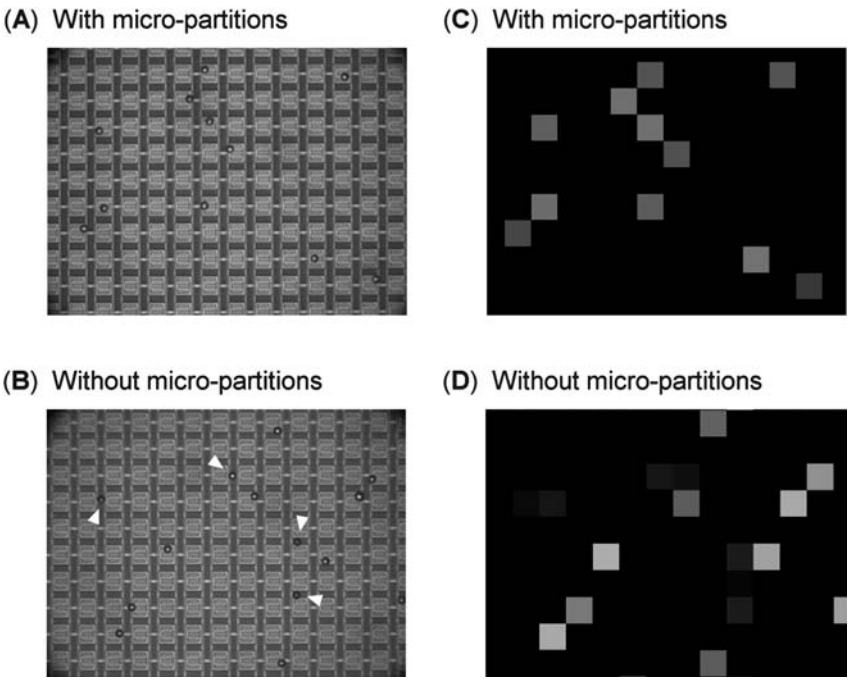

Fig. 4 Microscopic (A and B) and photosensor (C and D) images of HRP-particles on the TFT photosensor with (A and C) and without (B and D) micro-partitions.

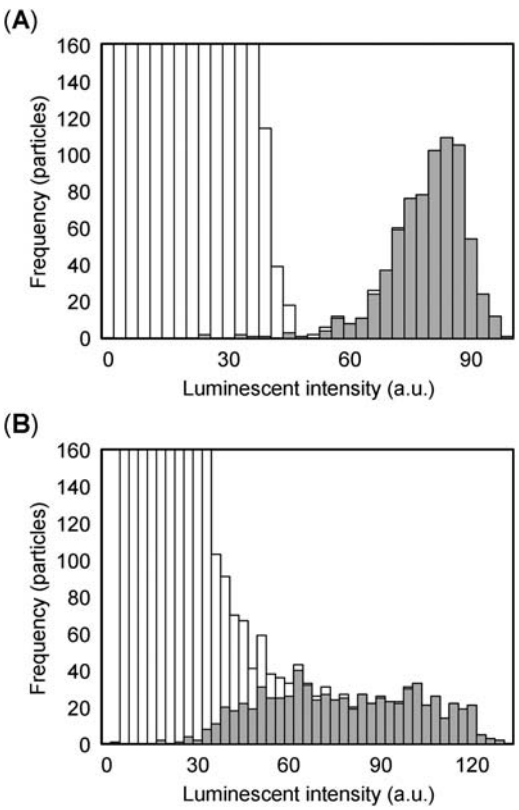

Fig. 5 Histograms of luminescent intensities measured by pixels of the TFT photosensor with (A) and without (B) micro-partitions. Exposure time was set at 4.8 s. (Grey column) Luminescent signals of HRP-particles. (White column) Background signals.

luminescent intensities of HRP-particles on the untreated TFT photosensor (Fig. 5B). These signals were not distinguishable from background. The signals from HRP-particles on gap spaces were detected by several pixels, resulting in an increase in background signals and a decrease in luminescent signals. We can conclude from these data that the fabrication of micro-partitions on the TFT photosensor allows highly accurate entrapment, counting, and luminescence-based detection of HRP-particles. A slight overlap between both histograms of luminescent intensities of the HRP-particles and the background signals was observed in the presence of micro-partitions. One of main possible reasons for this could be the higher background due to light detection by empty pixels nearby HRP-particles. Therefore, data analysis programs, which automatically subtract these background signals, should be developed in future work.

Detection of JM cells stained with mouse anti-human CD8 IgG1 antibody and HRP-labeled secondary antibody by the micro-partitioned TFT photosensor

The microfluidic TFT photosensor (micro-partitioned TFT photosensor integrated into microfluidic chamber) was used for the detection of JM cells stained with mouse anti-human CD8 IgG1 primary antibody and HRP-labeled anti-mouse IgG1 secondary antibody. One of the main advantages of the microfluidic TFT photosensor is to monitor the time-dependent light signal changes derived from single-cells entrapped between micro-partitions. Therefore, a real-time imaging of JM cells based on chemiluminescence was investigated (Fig. 6). Just before substrate introduction, no signals were detected (Fig. 6A). However, as the substrate spread to the end of the microfluidic channel, bright pixels were observed along the microfluidic channel (Fig. 6B and C). These bright pixels were derived from HRP-labeled JM cells entrapped on the pixels, which was

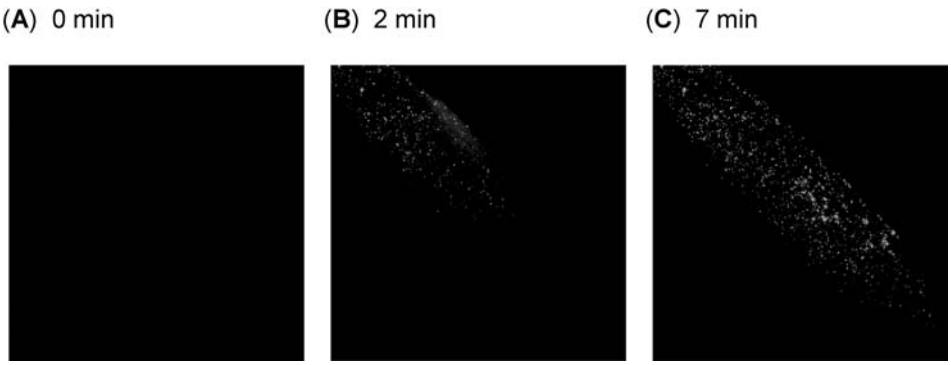

Fig. 6 Visualization of JM cells stained with mouse anti-human CD8 IgG1 primary antibody and HRP-labeled anti-mouse IgG1 secondary antibody using the microfluidic TFT photosensor. Chemiluminescent signals were measured every 30 s with constant introduction of the substrate solution. Exposure time was set at 21.0 s. The substrate solution flowed from the inlet (upper left) to the outlet (lower right). Full TFT photosensor images at 0 min (A), 2 min (B) and 7 min (C) after the beginning of substrate introduction.

confirmed by microscopic observation. These results indicate that entrapment of JM cells on the photosensor surface and luminescence-based detection was successfully achieved.

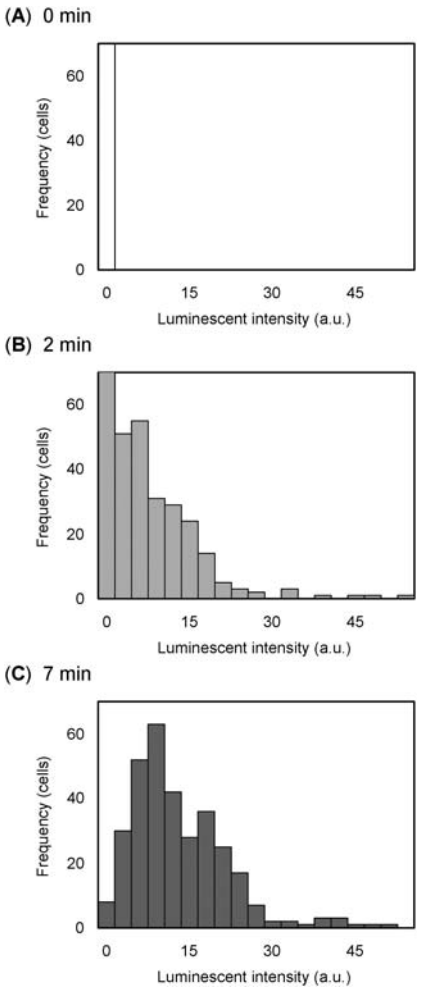

Fig. 7 Histograms of luminescent intensities of JM cells stained with mouse anti-human CD8 IgG1 primary antibody and HRP-labeled anti-mouse IgG1 secondary antibody measured by the microfluidic TFT photosensor at 0 min (A), 2 min (B) and 7 min (C) after the beginning of substrate introduction. Approximately, 300 cells were analyzed.

Although detection of HRP-labeled JM cells was accomplished as shown in Fig. 6, it also became obvious that part of the cells were entrapped on the same pixels. The efficiency of cell entrapment was mainly affected by cell concentration and flow rate. When 9.5×10^5 cells ml^{-1} of JM cells (10.0 μl) were introduced into the microfluidic chamber at a constant flow (3 μl min^{-1}), 5.4% of the photosensing areas of single pixels contained two or more JM cells. To overcome this obstacle to single-cell analysis, further downsizing of the photosensing area formed by the micro-partitions should be investigated in future work because an area of 30 μm × 30 μm is slightly too large for entrapment of single JM cells, which are 10 to 15 μm in diameter. In this paper, relatively a lower concentration of cell samples was used to overcome the above problems.

Fig. 7 shows the histograms of luminescent intensities of HRP-labeled JM cells on the TFT photosensor at 0 min (Fig. 7A), 2 min (Fig. 7B) and 7 min (Fig. 7C) after substrate introduction. The highest peak of the histograms was shifted towards the right-hand side as time advanced. These results indicate that real-time monitoring of chemiluminescence from the JM cells was successfully accomplished. The average intensity of HRP-labeled JM cells at an exposure time of 21.0 s was 0.0 ± 0.0 (a.u.) at 0 min, 6.2 ± 7.8 (a.u.) at 2 min and 12.1 ± 8.6 (a.u.) at 7 min, respectively. Because the average intensity of HRP-particles (2.8×10^6 HRP-molecules/particle) was 78.3 ± 9.7 (a.u.) at an exposure time of 4.8 s (Fig. 5A), HRP molecules attached to each JM cell would be much lower than that value. Although quantitative analysis has not been evaluated due to higher backgrounds in empty pixels as mentioned above, signal intensities would be proportionate to the expression level of cell surface proteins by using data analysis programs which subtract these background signals.

Conclusions

We have proposed a novel single-cell detection system using a micro-partitioned TFT photosensor integrated into a microfluidic chamber. Fabrication of micro-partitions on the TFT photosensor surface allows highly efficient single-cell entrapment of JM cells. The luminescent signals from individual cells were successfully recognized every 30 s by bright-pixel patterns, demonstrating that our proposed system will allow

high-throughput and real-time analysis of more than 10^4 cells with minimum optical system requirements. This is the first report of single-cell entrapment and subsequent signal detection on the photosensing area of individual pixels of TFT photosensors.

Acknowledgements

This work was funded in part by a support program for technology development based on academic findings from The New Energy and Industrial Technology Development Organization. This work was also funded in part by the support program for improving graduate school education of "Human Resource Development Program for Scientific Powerhouse" from the Ministry of Education, Culture, Sports, Science, and Technology of Japan to Yoshihiko Sunaga. We are deeply grateful for the device provided by Casio Computer Co. Ltd.

Notes and references

1 D. Daria, M. D. Filippi, E. S. Knudsen, R. Faccio, Z. Li, T. Kalfa and H. Geiger, *Blood*, 2008, **111**, 1894–1902.
2 P. A. Sotiropoulou, S. A. Perez, M. Salagianni, C. N. Baxevanis and M. Papamichail, *Stem Cells*, 2006, **24**, 462–471.
3 M. Safford, S. Collins, M. A. Lutz, A. Allen, C. T. Huang, J. Kowalski, A. Blackford, M. R. Horton, C. Drake, R. H. Schwartz and J. D. Powell, *Nat. Immunol.*, 2005, **6**, 472–480.
4 H. Liu, M. Komai-Koma, D. Xu and F. Y. Liew, *Proc. Natl. Acad. Sci. U. S. A.*, 2006, **103**, 7048–7053.
5 A. S. Moreau, X. Jia, H. T. Ngo, X. Leleu, G. O'Sullivan, Y. Alsayed, A. Leontovich, K. Podar, J. Kutok, J. Daley, S. Lazo-Kallanian, E. Hatjiharissi, M. S. Raab, L. Xu, S. P. Treon, T. Hideshima, K. C. Anderson and I. M. Ghobrial, *Blood*, 2007, **109**, 4964–4972.
6 Z. Benderra, A. M. Faussat, L. Sayada, J. Y. Perrot, R. Tang, D. Chaoui, H. Morjani, C. Marzac, J. P. Marie and O. Legrand, *Clin. Cancer Res.*, 2005, **11**, 7764–7772.
7 E. P. Papapetrou, M. J. Tomishima, S. M. Chambers, Y. Mica, E. Reed, J. Menon, V. Tabar, Q. Mo, L. Studer and M. Sadelain, *Proc. Natl. Acad. Sci. U. S. A.*, 2009, **106**, 12759–12764.
8 K. Hasegawa, A. B. Cowan, N. Nakatsuji and H. Suemori, *Stem Cells*, 2007, **25**, 1707–1712.
9 W. T. Shearer, H. M. Rosenblatt, R. S. Gelman, R. Oyomopito, S. Plaeger, E. R. Stiehm, D. W. Wara, S. D. Douglas, K. Luzuriaga, E. J. McFarland, R. Yogev, M. H. Rathore, W. Levy, B. L. Graham and S. A. Spector, *J. Allergy Clin. Immunol.*, 2003, **112**, 973–980.
10 F. G. Behm, S. C. Raimondi, M. J. Schell, A. T. Look, G. K. Rivera and C. H. Pui, *Blood*, 1992, **79**, 1011–1016.
11 M. Keeney, I. Chin-Yee, K. Weir, J. Popma, R. Nayar and D. R. Sutherland, *Cytometry*, 1998, **34**, 61–70.
12 M. M. Wang, E. Tu, D. E. Raymond, J. M. Yang, H. Zhang, N. Hagen, B. Dees, E. M. Mercer, A. H. Forster, I. Kariv, P. J. Marchand and W. F. Butler, *Nat. Biotechnol.*, 2005, **23**, 83–87.
13 Y. C. Tung, Y. S. Torisawa, N. Futai and S. Takayama, *Lab Chip*, 2007, **7**, 1497–1503.
14 H. N. Joensson, M. L. Samuels, E. R. Brouzes, M. Medkova, M. Uhlen, D. R. Link and H. Andersson-Svahn, *Angew. Chem., Int. Ed.*, 2009, **48**, 2518–2521.
15 J. R. Kovac and J. Voldman, *Anal. Chem.*, 2007, **79**, 9321–9330.
16 T. Matsunaga, M. Hosokawa, A. Arakaki, T. Taguchi, T. Mori, T. Tanaka and H. Takeyama, *Anal. Chem.*, 2008, **80**, 5139–5145.
17 M. Hosokawa, A. Arakaki, M. Takahashi, T. Mori, H. Takeyama and T. Matsunaga, *Anal. Chem.*, 2009, **81**, 5308–5313.
18 D. Wlodkowic, S. Faley, M. Zagnoni, J. P. Wikswo and J. M. Cooper, *Anal. Chem.*, 2009, **81**, 5517–5523.
19 A. Ozcan and U. Demirci, *Lab Chip*, 2008, **8**, 98–106.
20 T. W. Su, S. Seo, A. Erlinger and A. Ozcan, *Biotechnol. Bioeng.*, 2009, **102**, 856–868.
21 S. Seo, T. W. Su, D. K. Tseng, A. Erlinger and A. Ozcan, *Lab Chip*, 2009, **9**, 777–787.
22 S. Moon, H. O. Keles, A. Ozcan, A. Khademhosseini, E. Haeggstrom, D. Kuritzkes and U. Demirci, *Biosens. Bioelectron.*, 2009, **24**, 3208–3214.
23 T. Tanaka, K. Hatakeyama, M. Sawaguchi, A. Iwadate, Y. Mizutani, K. Sasaki, N. Tateishi, H. Takeyama and T. Matsunaga, *Biotechnol. Bioeng.*, 2006, **95**, 22–28.
24 K. Hatakeyama, T. Tanaka, M. Sawaguchi, A. Iwadate, Y. Mizutani, K. Sasaki, N. Tateishi and T. Matsunaga, *Lab Chip*, 2009, **9**, 1052–1058.

